COBEM 2021 26th International Congress of Mechanical Engineering
November 22-26, 2021, Virtual Congress, Brazil

COB-2021-1729
DYNAMIC BEHAVIOUR OF A REDUCED HEAVE MOTION PLATFORM FOR OFFSHORE WIND TOWER

Paulo Oliveira Kiryu*
Celso Kazuyuki Morooka
Marcelo Anunciação Jaculli
University of Campinas, Faculty of Mechanical Engineering & Center of Petroleum Studies, Campinas-SP, Brazil
* p137245@dac.unicamp.br

Bernt Johan Leira
Sigbjørn Sangesland
Norwegian University of Science and Technology, Trondheim, Norway

Abstract. *A new type of floating platform has been investigated. It is a small monocolumn semi-submersible floating platform with an internal air chamber that contributes to reduce platform vertical motions. It enables offshore wind tower to operate in deepwater, although a good performance can be also expected in harsh environmental conditions such as those seen in the North Sea. The power generated from the offshore wind system can supply electric power to run the oil and gas production equipment such as those in the process plant, platform facilities as well as those systems at the seabed. In this work, numerical simulations of platform motions are conducted with the aid of a previously developed formulation. Results for heave motions are shown considering scenarios with and without the air chamber effect and the mooring system. It has been verified that this new platform indeed experiences smaller motions which can increase the effectiveness of the wind power generation and improve the safety of operations.*

Keywords: *floating platform, offshore petroleum, wind energy, ocean waves, mooring system*

1. INTRODUCTION

In the recent years, a great demand for energy is being observed worldwide. Each country shows its own solution to overcome this demand, although a tendency of the preference for renewable energy is increasingly observed. A similar trend is also observed in Brazil where the oil and gas industry should play an important contribution by extending their business target to energy.

The offshore petroleum industry has been developed and accumulated a large amount of knowledge for designing and operating floating production systems (FPS) in deep-water. This expertise might be determinant for the build and operation of offshore wind systems. A motivation to operate an offshore wind farm together with the oilfield production in deep-water is the possibility to replace, partially or totally, the electricity and other energy need to run oil and gas production equipment. Moreover, it would contribute to the relief of CO2 and NOx emissions (Shadman *et al*., 2020) with contributions to the sustainability of the environment.

Although, aspects of the conceptual design of a floating production platform for oil gas production need to be reviewed and adapted to suit as a support of a Floating Offshore Wind Turbine (FOWT). For instance, there is an important need to investigate platform motion dynamics in waves and mooring system design due to difference on size of a FOWT platform if compared with an FPS.

In the last years, the literature is gaining more studies regarding concepts of FOWT for deep waters. Most of these concepts are Spar (mono column), Semi-submersible or Tension-leg type platforms. Different issues of FOWT have been investigated. Suzuki *et al*. (2019) investigated, experimentally and numerically, the elastic response characteristics of a lightweight floating support structure of a FOWT with guywire supported tower, looking for the basic load transmission mechanism. Chuang *et al*. (2021) also studied, numerically and experimentally, a moored floating barge moonpool platform equipped with an NREL 5 MW wind turbine under wave and wind loads, and they analyzed the hydrodynamic performance and stability of the barge platform and the mooring system, and one important conclusion is the key issue of the mooring system in the shallow water condition.

Floating platform motions reducing mechanisms have been also investigated. Kurniawan *et al*. (2014) analyzed different wave energy devices which have compressible submerged volumes of air in which horizontal air-water surface is free to move vertically relative to the device. The linear potential theory in frequency domain was used. Their initial analysis included bodies with no power take-off (PTO) system to demonstrate the effects of a compressible volume on

the body response. They concluded that the hydrostatic stiffness is lowered leading to longer resonance periods. Midtbust (2018) studied a new concept of monocolumn platform with a submerged pneumatic air chamber to maintain constant buoyancy and reduce the vertical motion. He concluded that the air chamber can reduce the motion for some regular wave frequencies, and the modeling needs to be much improved, i.e., thermodynamic aspects and non-linearity effects of the chamber. Different geometries for a monocolumn platform for supporting oil and gas operations have been also studied by Jaculli *et al.* (2020), and they proposed a motion dynamics model and performed calculations of the motion with and without air chamber. They concluded that the air chamber reduced the heave motion for some of the geometries investigated.

In the present work, a monocolumn type platform is proposed as a floating base for FOWT in deep water. The platform is provided with closed air chambers around columns below the platform deck with the purpose to minimize platform motions, particularly in the vertical direction. Dynamic behavior of the platform in vertical direction with air chamber is described, and numerical simulations of the vertical motion are carried out with and without mooring system effects.

2. DYNAMIC BEHAVIOR OF THE PLATFORM

2.1 Equation of Motions

In general, the six degrees of motion freedom of a floating platform (Vardaro *et al.*, 1995; Ishihara *et al.*, 2001) can be written as follows:

$$\sum_{j=1}^{6}(\boldsymbol{M}_{ij} + \boldsymbol{a}_{ij})\ddot{\boldsymbol{x}}_j + \boldsymbol{b}_{ij}\dot{\boldsymbol{x}}_j + \boldsymbol{C}_{ij}\boldsymbol{x}_j = \boldsymbol{F}_i(t), i = 1, 2, \dots, 6 \quad (1)$$

where, $\boldsymbol{M}$: inertia matrix; $\boldsymbol{a}$: added mass matrix; $\boldsymbol{b}$: potential damping matrix; $\boldsymbol{C}$: hydrostatic restoring matrix; and $\boldsymbol{F}$: exciting external force.

From the above equation, if the vertical heave motion of the platform is taken nondependent of other motions, it can be written as in the following Eq. (2):

$$(M_{33} + a_{33})\ddot{x}_3 + b_{33}\dot{x}_3 + C_{33}x_3 = F_3(t) \quad (2)$$

where, M_{33}: inertia in heave; a_{33}: added mass in heave; b_{33}: potential damping in heave; C_{33}: hydrostatic restoring in heave; and F_3: exciting external force in heave.

Figure (1) shows a scheme for the moored FOWT.

The force caused by the air chamber in the Eq. (2) can be added by F_{ch}, as follows:

$$(M_{33} + a_{33})\ddot{x}_3 + b_{33}\dot{x}_3 + C_{33}x_3 + F_{ch} = F_3 \quad (3)$$

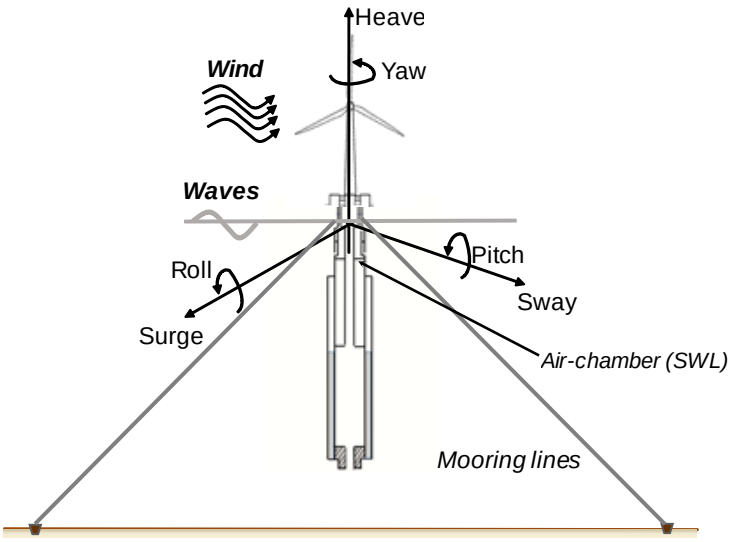

Figure 1. Scheme for the moored floating platform at the initial equilibrium.

2.2 The Air Chamber

The air chamber force comes from changes in the volume of air contained in the chamber. It can be represented as a linear spring with a stiffness (C_{33g}) as the Hooke's law, as shown in Eq. (4).

$$F_{ch} = C_{33g} x_{3int} = A_g \rho_w g x_{3int} \tag{4}$$

Based on previous results shown in Jaculli *et al*. (2020), Eq. (3) and Eq. (4) can be written as in Eq. (5):

$$\left(M_{33} + a_{33}(\omega)\right)\ddot{x_3} = -b_{33}(\omega)\dot{x_3} - A_w \rho_w g x_3 - A_g \rho_w g x_{3int} + F(\omega)\zeta \tag{5}$$

where, ω is the circular frequency, $a_{33}(\omega)$ is the added mass, $b_{33}(\omega)$ is the damping, A_w is the cross-sectional area at the sea level (annular area, already consider the subtraction of moonpool area), g is gravity, ρ_w is the water density, A_g is the air chamber cross-sectional area (annular), x_3 is the platform vertical motion, x_{3int} is the vertical change in the air-water interface in the chamber entrance (in relation to the platform), $F(\omega)$ is the heave hydrodynamic excitation force and ζ is the sea elevation. ζ can be simplified to $\zeta = \zeta_a \cos(\omega t)$, for regular waves (Faltinsen, 1990). The frequency-dependent quantities (a_{33}, b_{33}, and F) are calculated with potential flow theory, with the use of commercial software.

To calculate x_3 and x_{3int}, another equation is needed. Inside the air chamber, the instantaneous pressure p is:

$$p = p_0 + \rho_w g\left(\zeta e^{-k_w(H_0 - L_0 - x_3 - x_{3int})} - x_3 - x_{3int}\right) \tag{6}$$

where, p_0 is the initial air pressure, k_w is the wave number, and H_0 and L_0 are dimensions related to chamber entrance. The exponential term in Eq. (6) of the dynamic pressure at the air chamber considers the platform heave motion and the incident regular wave effects. And, by accounting the instantaneous air chamber volume in the equation of the gas law, it follows as in Eq. (7).

$$p \cdot \left(V_0 - A_g x_{3int}\right) = Z m_a R_a T_0 \tag{7}$$

where, V_0 is the initial volume of air (given), Z is the compressibility factor, m_a is the mass, R_a is the gas constant and T_0 is the initial temperature. From the Equations (5), (6), and (7), x_3, x_{3int}, and p can be obtained as in Jaculli *et al*. (2020), and the system of algebraic differential equations of the problem are summarized in Eq. (8). Solution of the system of equations in Eq. (8) can be numerically achieved by a time-stepping approach such as the Runge-Kutta method, and finally, the vessel heave motion x_3 is obtained.

$$\begin{Bmatrix} \frac{-A_w \rho_w g x_3 - b_{33}(\omega)\dot{x_3} - A_g \rho_w g x_{3int} + F(\omega)\zeta}{M_{33} + a_{33}(\omega)} \\ -\rho_w g x_3 - \rho_w g x_{3int} - p + p_0 + \rho_w g \zeta e^{-k_w(H_0 - L_0 - x_3 - x_{3int})} \\ A_g x_{3int} p - V_0 p + Z m_a R_a T_0 \end{Bmatrix} = \begin{Bmatrix} \ddot{x_3} \\ 0 \\ 0 \end{Bmatrix} \tag{8}$$

The dynamic behavior of the coupled floating platform system as in the above Eq. (8) might follow nonlinear response for the heave motion. Nonlinearities in heave motion are expected due to compression of the confined air in the chamber through heave restoring forces and damping effects. Although, small amplitude heave motion is considered, and for long wave periods small amplitude heave motion is expected when the vertical motion is almost in phase with the incident wave with small amplitude. In order to obtain the platform Response Amplitude Operation (RAO), linearization was taken in Equations (5) to (7) for air chamber effects by using equivalent air chamber stiffness (C_{33eq}). This stiffness is obtained considering the platform mean initial position at the equilibrium. Midtbust (2018) proposed this linearization as in Eq. (9), where air dynamic compression effects are disregarded. RAO of the heave motion are compared with results obtained by the linear potential theory.

$$C_{33eq} = \frac{\gamma p_0 A_g^2}{V_0} \tag{9}$$

where, γ is the polytrophic constant for the air. With C_{33eq}, the dynamic pressure is converted to a restoring force:

$$(p - p_0)A_g = C_{33eq} x_{3int} \;\rightarrow\; p = \frac{\gamma p_0 A_g}{V_0} x_{3int} + p_0 \tag{10}$$

Substituting this result into Eq. (6) we obtain:

$$x_{3int} = -\frac{\rho_w g}{\left(\frac{\gamma p_0 A_g}{V_0} + \rho_w g\right)}\left(x_3 - \zeta e^{-k_w(H_0 - L_0 - x_3 - x_{3int})}\right) \tag{11}$$

The exponential term in the above Eq. (11), nearby the zero frequency (long waves), can be approximated to the unity, only remaining the sea surface wave elevation ζ. Then, if the Eq. (11) is considered into Eq. (5), we can obtain the Eq. (12) with the unknown variable x_3:

$$(M_{33} + a_{33})\ddot{x_3} + b_{33}\dot{x_3} + \left[A_w \rho_w g - \frac{A_g \rho_w^2 g^2}{\left(\frac{\gamma p_0 A_g}{V_0} + \rho_w g\right)}\right] x_3 = \left[F(\omega) - \frac{A_g \rho_w^2 g^2 e^{-k_w(H_0 - L_0)}}{\left(\frac{\gamma p_0 A_g}{V_0} + \rho_w g\right)}\right]\zeta \tag{12}$$

According to this equation, the air chamber modifies the hydrostatic restoring coefficient reducing the stiffness of the platform, and the natural frequency decreases. It was also observed in Jaculli *et al*. (2020). Besides, the excitation force caused by the waves is also reduced.

Harmonic solution $x_3(t) = x_{3a} \exp(i\omega t)$ is considered for the Eq. (12), where x_{3a} is the amplitude of heave motion $x_3(t)$. The total equivalent restoring coefficient C_{33rest} is given by:

$$C_{33rest} = A_w \rho_w g - \frac{A_g \rho_w^2 g^2}{\left(\frac{\gamma p_0 A_g}{V_0} + \rho_w g\right)} \tag{13}$$

Then, Eq. (14) is obtained by applying the harmonic solution into Eq. (12), and finally, the RAO and its phase ϕ is achieved as in the Eq. (15) and (16), respectively.

$$[-\omega^2(M_{33} + a_{33}) + i\omega b_{33} + C_{33rest}]x_{3a} = \left[F(\omega) - \frac{A_g \rho_w^2 g^2 e^{-k_w(H_0 - L_0)}}{\left(\frac{\gamma p_0 A_g}{V_0} + \rho_w g\right)}\right]\zeta \tag{14}$$

$$RAO = \left|\frac{x_{3a}}{\zeta}\right| = \frac{F(\omega) - \frac{A_g \rho_w^2 g^2 e^{-k_w(H_0 - L_0)}}{\left(\frac{\gamma p_0 A_g}{V_0} + \rho_w g\right)}}{\sqrt{[C_{33rest} - (M_{33} + a_{33})\omega^2]^2 + (b_{33}\omega)^2}} \tag{15}$$

$$\phi = \arctan \frac{\frac{b_{33}\omega}{C_{33rest}}}{1 - \frac{(M_{33} + a_{33})\omega^2}{C_{33rest}}} \tag{16}$$

The numerator in the last term in Eq. (15) can be taken as $F(\omega) + C_{33rest} - A_w \rho_w g$ for very long wave periods because the exponential term becomes near 1. In this condition, variations of the sea level become almost quasi-static, and the heave exciting force is simply $A_w \rho_w g \zeta$. Then, $F(\omega)$ and $A_w \rho_w g$ will cancel out ($F(\omega)$ is the force per unit wave amplitude) by reducing the numerator to C_{33rest} at zero frequency. Therefore, if the platform geometry is taken such that $C_{33rest} \approx 0$, the principle of buoyancy counterbalancing can be observed as in Midtbust (2018) in the platform modeling in the present study. Including the mooring stiffness into Equations (13) and (15) follows that:

$$C_{33rest,m} = A_w \rho_w g + C_{33m} - \frac{A_g \rho_w^2 g^2}{\left(\frac{\gamma p_0 A_g}{V_0} + \rho_w g\right)} \tag{17}$$

$$RAO = \left|\frac{x_{3a}}{\zeta}\right| = \frac{F(\omega) - \frac{A_g \rho_w^2 g^2 e^{-k_w(H_0 - L_0)}}{\left(\frac{\gamma p_0 A_g}{V_0} + \rho_w g\right)}}{\sqrt{\left[C_{33rest,m} - (M_{33} + a_{33})\omega^2\right]^2 + (b_{33}\omega)^2}} \tag{18}$$

2.3 Hydrodynamic force and coefficients and mooring effects

Wave forces and hydrodynamic coefficients of the platform were calculated based on the linear potential theory through Wadam (DNV-GL, 2018). For the sake of simplicity, the air-water interface in the air chamber for the hydrodynamic problem was modeled as a fixed plate. Hydrodynamic wave forces and coefficients were calculated in frequency-domain, and numerical simulations were obtained based on equations described in section 2.2.

Hydrodynamic forces and coefficients for heave motion are shown below, where the mark "~" denotes the dimensionless coefficient given by as follows:

$$a_{33} = (\rho_w V_v)\tilde{a}_{33} \tag{19}$$

$$b_{33} = \left(\rho_w V_v \sqrt{\frac{g}{L}}\right) \tilde{b}_{33} \tag{20}$$

$$F_3 = \left(\frac{\rho_w V_v g}{L}\right) \tilde{F}_3 \tag{21}$$

Mooring system acts as an additional platform restoring stiffness, and in the present analysis, to simplify the mooring system stiffness, it is represented as a linear spring. Then, in Eq. (5), the mooring term C_{33m} can be added to the hydrostatic restoring coefficient, leading to:

$$\left(M_{33} + a_{33}(\omega)\right)\ddot{x}_3 = -b_{33}(\omega)\dot{x}_3 - (A_w \rho_w g + C_{33m})x_3 - A_g \rho_w g x_{3int} + F(\omega)\zeta \tag{22}$$

Therefore, C_{33m} is provided as a multiple of the hydrostatic restoring coefficient in the form $C_{33m} = f_m A_w \rho_w g$ where f_m is defined as the mooring factor, where $0 \leq f_m \leq 2$ to show the mooring effects in two-dimensional surfaces of RAO in the results.

A Runge-Kutta time-stepping algorithm was applied for the time domain integration, and a computer code was implemented in MATLAB® to obtain $x_3(t)$.

3. RESULTS AND DISCUSSIONS

A parametric study by numerical simulations was conducted to investigate motion behavior of the FOWT. As the first step of this study, different geometries for the platform (Platform 1, 2, and 3) were verified, among those to verify effects of the air chamber in the heave motion reduction of the platform and observing effects from the moonpool geometry. In the present work, results for the Platform 2, with uniform regular moonpool (Figure 2) are shown. Regular waves are considered and we obtain results calculated by linearized closed formulas for the heave RAO, and results by time domain simulations in which nonlinearities are included. Hydrostatic restoration due to the air chamber and effects of the mooring system had also been verified in the calculations. Table 1 shows the main dimensions of the platform in the simulations, and Figure 2 an overview of Platform 2 geometry.

Table 1. Main dimensions of the Platform 2.

Dimension	Value	Unit
Diameter at sea level (D_w)	8.37	m
Cross-sectional area at the sea level (A_w)	18.70	m^2
Air chamber cross-sectional area (A_g)	34.95	m^2
Total length of structure	109.00	m
Draft	100.00	m
H_0	12.90	m
L_0	4.45	m
Wave amplitude input (ζ_a)	1	m
Characteristic length input (L)	100	m
Gravity (g)	9.807	m/s^2
Sea water density (ρ_w)	1025	kg/m^3
Submerged volume (V_v)	16151	m^3

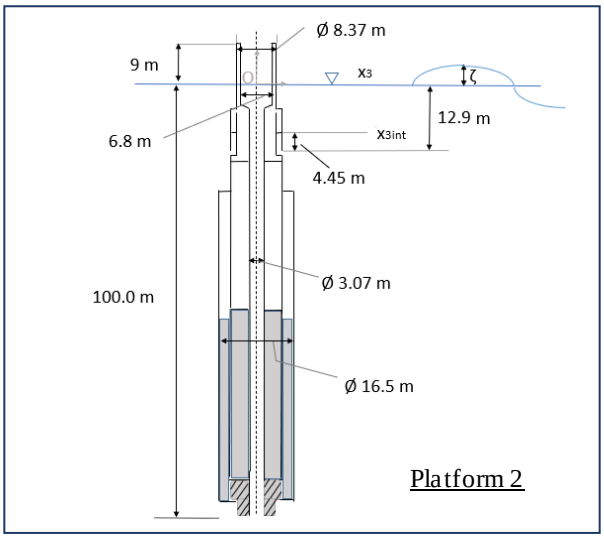

Figure 2. Geometry of Platform 2.

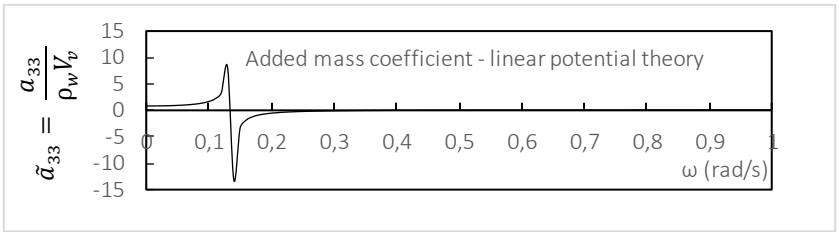

Figure 3. Dimensionless heave added mass coefficient as a function of circular frequency, in rad/s.

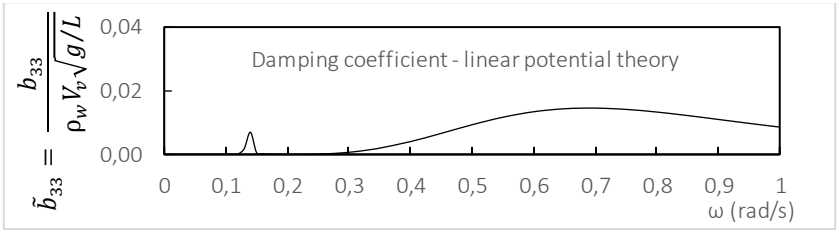

Figure 4. Dimensionless heave damping coefficient as a function of circular frequency, in rad/s.

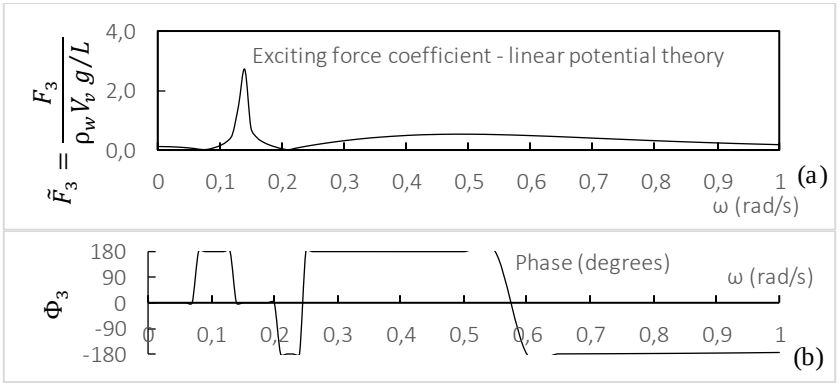

Figure 5. Dimensionless heave exciting force coefficient (a) and phase (b) as a function of circular frequency, in rad/s.

Hydrodynamic coefficients, wave forces, and RAOs from the linear potential theory were calculated. A frequency range from $\omega \approx 0$ rad/s to $\omega = 1.0$ rad/s (wave period of 6.28 s) was considered. Although, very low frequency ω close to zero was investigated to observe the counterbalancing of the buoyancy (Midtbust, 2018).

Moreover, the heave RAO as in Eq. (15), for platform motion without the air chamber, was obtained by the implemented computer code and compared with results from the linear potential theory (Wadam). Finally, calculations in the time-domain have been performed by following Eq. (8).

Hydrodynamic added mass and damping, and the wave exciting force for the heave, in non-dimensional form, of Platform 2 are respectively shown in Figures 3, 4, and 5. Sudden changes are observed in the hydrodynamic coefficients and wave forces in the $\omega \approx 0.14$ rad/s, where for instance, we can observe negative added mass which should be due the existence of two main diameters along the moonpool length.

The heave RAO obtained from the linear potential theory for the platform without the air chamber is shown in Figure 6. A resonance peak can be observed around $\omega \approx 0.19$ rad/s. RAO from the linearized model for the air chamber without platform mooring is also shown in Figure 6. For the no air chamber case, the terms of the air chamber are discarded from Eq. (15).

Observing the RAO in the Figure 6, the "no air chamber and no mooring" result matches very well with the RAO from the linear potential theory, which verifies observation in the Eq. (15) when $A_g\rho_w g = 0$ kN/m. Moreover, the air chamber effect reduces the equivalent stiffness of the system and its natural frequency, which can be noted by comparing the "only chamber" results with other results. This effect is important because the resonance peak should be tuned far away from the range of wave frequencies seen in the sea (0.2 ~ 1.0 rad/s), also observed by Kurniawan *et al.* (2014).

It is also important to observe motion amplitude in quasi-static behavior nearby the zero frequency which could correspond to the tides. In general, the RAO of most of the offshore ships and platforms approximate to unity for lower frequencies (heave motion equals to the increase in water level), as the cases of "no chamber no mooring" curve and "linear potential theory" curve. The heave response of the platform with air chamber deviates from the usual unity RAO value, when the incident wave frequency approaches zero due to the principle of buoyancy counterbalancing effects (Midtbust, 2018).

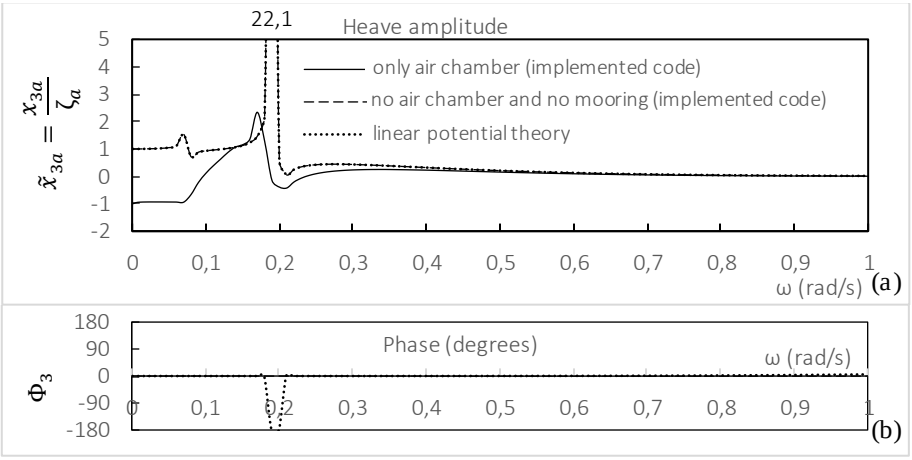

Figure 6. RAO (a) and phase (b) comparison for heave amplitude as a function of circular frequency, in rad/s.

Mooring effects in the heave motion resonance peak and amplitudes are observed through Eq. (18). Two-dimensional response surfaces in the function of mooring and regular wave frequencies are used to visualize results. Figures 7 and 8 show heave motion responses of the platform for with and without the air chamber cases, respectively. Heave response surfaces are shown against the wave frequency and different values for the mooring stiffness. Some portions of the response surface have been cut to enhance the overview of heave motion behavior overall. The value of C_{33rest} is not exactly zero ($C_{33rest} \approx 0.64$ kN/m), but it is much smaller than the value of $A_w\rho_w g$.

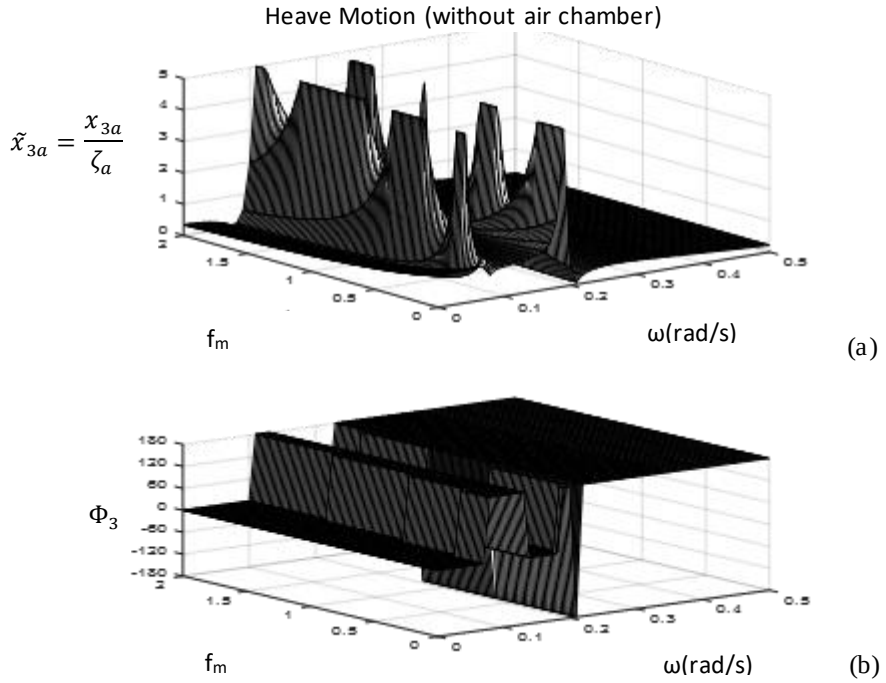

Figure 7 Heave motion calculated by implemented computer code without air chamber with mooring. (a) Amplitude (b) Phase.

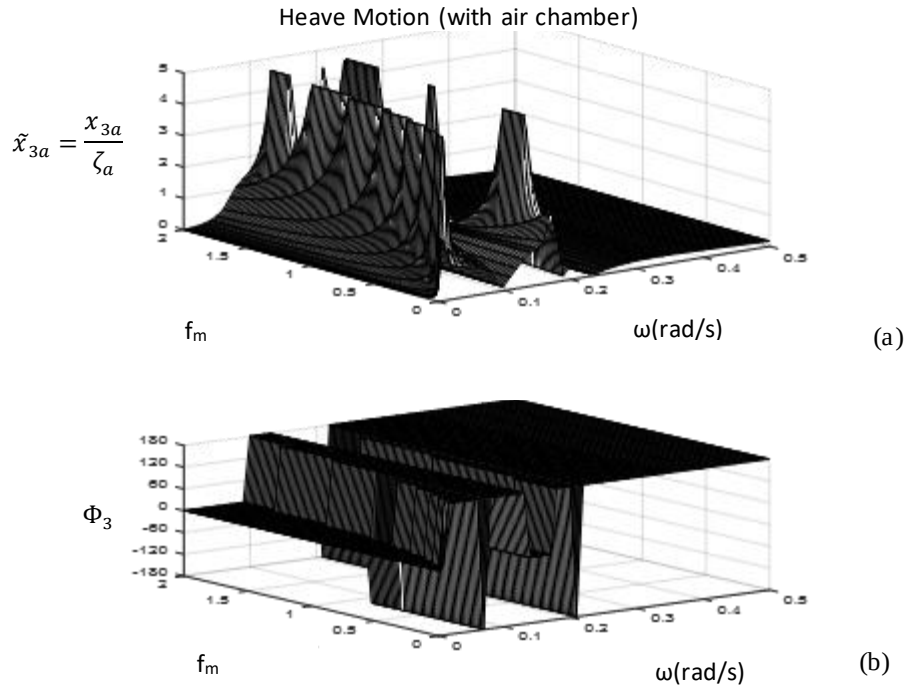

Figure 8. Heave motion calculated by implemented computer code with air chamber with mooring. (a) Amplitude (b) Phase.

An interesting result is the RAO at low wave frequencies in the case with the air chamber and mooring that approximate to zero. This is due to the cross-sectional area of the platform water-plane area (A_w) reduced according to Table 1, in order to set the total equivalent restoring coefficient of Platform 2 near to zero ($C_{33rest} \approx 0$ kN/m). In that case, the buoyancy counterbalancing effect is seen (Midtbust, 2018). It can be added that the air chamber effects interact with the mooring restoring effects for the heave motion stabilization in this range of wave frequencies. We can also observe that the mooring restoring increases the heave resonance peak frequency, as expected.

The time series with nonlinearities from the chamber included obtained from the solution of Eq. (8) are shown in Figure 9 (a) to (c). Time series for regular waves for three typical wave periods and a flat value of $\zeta_a = 6$ m were used. Mooring system ($f_m = 2$) was taken on those time series and results are shown by comparing cases with and without air chamber.

A comparison of motion can be done between the RAO from Eq. (18) and the mean value of the amplitudes of platform motion from the time-series, with added mooring to stabilize the numerical convergence of that solution and reduce the heave motion. Here, the wave period of 7 s (0.9 rad/s), 15 s (0.42 rad/s), and 20 s (0.31 rad/s), were chosen because it is common period seen in the sea. According to Figure 9 the air chamber reduced the heave motion, for example, for wave period of 15 s, the mean amplitude without air chamber is 2.63 m and with it is 1.94 m. For 20 s, this amplitude without air chamber is 4.53 m and with it is 2.81 m.

Despite the incident regular wave, two main frequencies can be observed in the heave time series. One frequency following the incident wave frequency and another one close to the platform heave natural frequency which might happen due to the underestimated heave damping with no viscous effects included.

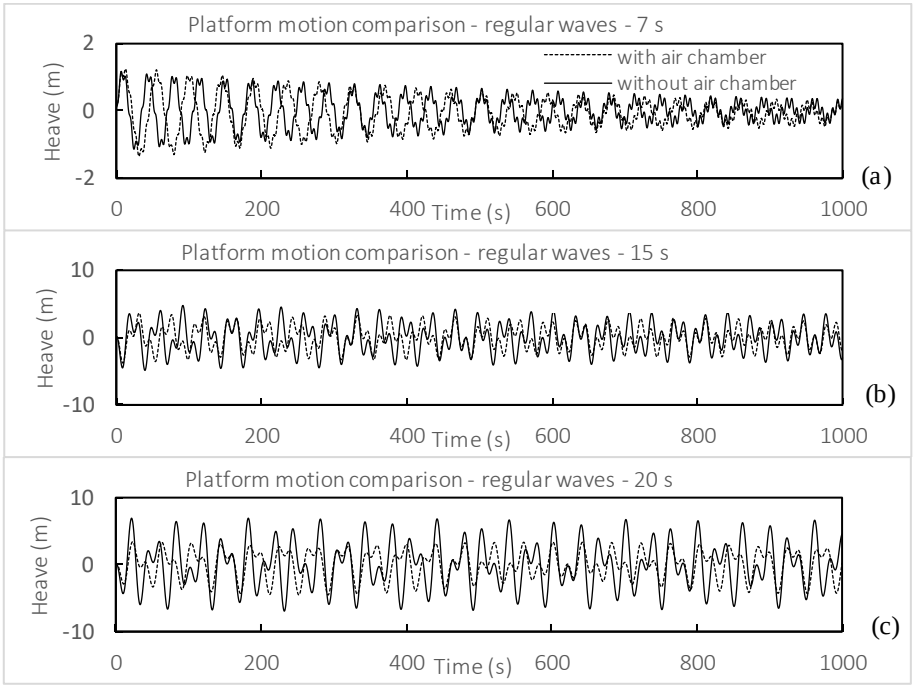

Figure 9. Time series for the nonlinear solution due to air chamber in regular waves by the implemented computer code. (a) 7 s; (b) 15 s; (c) 20 s.

4. CONCLUSIONS

A monocolumn type platform is proposed as a floating base to support a tower for the offshore wind turbine in deep water. A platform provided with closed air chambers around columns below the main deck is considered to reduce platform motions in the vertical direction. Dynamic effects of the air chamber and mooring system restoring were investigated through numerical simulation for the vertical platform motions.

Formulations for the Response Amplitude Operator (RAO) and nonlinear response of the heave were obtained for the monocolumn FOWT with air chamber to reduce vertical motions. Results were compared in frequency-domain with solutions from the linear potential theory (Wadam).

From the results, it is observed that the air chamber effect reduces the natural frequency of the platform heave motion while the mooring system effect moves it to higher frequencies. This tendency can be used to fit the design of the FOWT. Another interesting observation from the results was that the buoyancy counterbalancing effect from the air chamber for the long wave periods makes the RAO tend to zero, although mooring effect is determinant in this process.

Finally, interesting linear and nonlinear solutions were obtained for a monocolumn FOWT with reduced heave motion due to air chamber effects. The air chamber reduces the heave motion and the mooring restoring effects add benefits to the heave motion behavior performance. Formulations can be useful a faster tool in the preliminary design of this type of platform including the mooring system effects.

As a future work, more investigation will be extended for other platform motions, particularly for the pitch motions, and verify in deep, viscous effects involved in the platform motions.

5. ACKNOWLEDGMENTS

The authors would like to acknowledge The Research Council of Norway for funding the Brazilian-Norwegian Subsea Operations Consortium through the INTPART program, which supports the ongoing international cooperation between the Norwegian University of Science and Technology and the University of Campinas. The second author would like to thank the Coordination for the Improvement of Higher Education Personnel (CAPES), Print 88887.310645/2018-00; and the Brazilian National Council for Scientific and Technological Development (CNPq), 308551/2017-6, for their support. Also, we acknowledge Per Vatne for originally proposing this platform concept, which was given the name "StationMar".

6. REFERENCES

Chuang, T., Yang, W., and Yang, R., 2021. "Experimental and numerical study of a barge-type FOWT platform under wind and wave load". *Ocean Engineering*, Vol. 230. No.1 pp. 109015

DNV-GL, 2018. *Sesam user manual, Wadam.*

Faltinsen, O. M., 1990. *Sea Loads on Ships and Offshore Structures*. Cambridge University Press, Cambridge.

Ishihara, C.T., Batelochi, G.J., and Morooka, C.K., 2001. "Simulation of Floating Production Platform Motions in Directional Waves". *In Proceedings of the 20th International Conference on Offshore Mechanics and Arctic Engineering – OMAE 2001*. Houston, USA.

Jaculli, M. A., Leira, B. J., Sangesland, S., Morooka, C. K., and Mendes, J. R. P., 2020. "Dynamic Behavior of a Novel Heave Compensated Floating Platform for Well Interventions". In *Proceedings of the 39th International Conference on Offshore Mechanics and Arctic Engineering – OMAE 2020*. Virtual.

Kurniawan A., Greaves D., and Chaplin J., 2014 "Wave energy devices with compressible volumes". *Proceedings of the Royal Society A Mathematical Physical and Engineering Sciences*, Vol. 470.

Midtbust, S.S., 2018. *Concept Study and Analysis of a Constant Buoyancy System for a Floating Single Column Platform.* Master's Thesis, Department of Marine Technology, Norwegian University of Science and Technology, Trondheim, Norway.

Vardaro, E., Morooka, C.K.,1995. "Simulations of Horizontal Motions of a Floating Platform Under Ocean Waves, Wind and Current". In *Proceedings of the 9th International Symposium on Offshore Engineering*. Rio de Janeiro, Brasil.

Shadman, M., Estefen, S.F., Nunes, K., Amiri, M.M., Tavares, L.F., Rangel, P., and Assad, L.P., 2020. "Offshore Wind-Powered Oil and Gas Fields: A Preliminary Investigation of the Techno-Economic Viability for the Offshore Rio de Janeiro". In *Proceedings of the 39th International Conference on Offshore Mechanics and Arctic Engineering – OMAE 2020*. Virtual.

Suzuki, H., Xiong, J., Carmo, L.H.S., Vieira, D.P., Mello, P.C., Malta, E.B., Simos, A.N., Hirabayashi, S., and Gonçalves, R.T., 2019. "Elastic response of a light-weight floating support structure of FOWT with guywire supported tower", *Journal of Marine Science and Technology*, Vol. 24, pp. 1015–1028.

7. RESPONSIBILITY NOTICE

The authors are the only responsible for the printed material included in this paper.